Published in final edited form as:
Cell. 2009 July 10; 138(1): 51–62. doi:10.1016/j.cell.2009.04.030.

WNT/TCF signaling through LEF1 and HOXB9 mediates lung adenocarcinoma metastasis

Don X. Nguyen[1], **Anne C. Chiang**[2], **Xiang H.F. Zhang**[1], **Juliet Y. Kim**[1], **Mark G. Kris**[2,5], **Marc Ladanyi**[3,4], **William L. Gerald**[3,4], and **Joan Massagué**[1,6]

[1] Cancer Biology and Genetics Program, Memorial Sloan-Kettering Cancer Center, New York, NY, USA

[2] Department of Medicine, Memorial Sloan-Kettering Cancer Center, New York, NY, USA

[3] Department of Pathology, Memorial Sloan-Kettering Cancer Center, New York, NY, USA

[4] Human Oncology and Pathogenesis Program, Memorial Sloan-Kettering Cancer Center, New York, NY, USA

[5] Weill Medical College of Cornell University, Memorial Sloan-Kettering Cancer Center, New York, NY, USA

[6] Howard Hughes Medical Institute, Memorial Sloan-Kettering Cancer Center, New York, NY, USA

Summary

Metastasis from lung adenocarcinoma can occur swiftly to multiple organs within months of diagnosis. The mechanisms that confer this rapid metastatic capacity to lung tumors are unknown. Activation of the canonical WNT/TCF pathway is identified here as a determinant of metastasis to brain and bone during lung adenocarcinoma progression. Gene expression signatures denoting WNT/TCF activation are associated with relapse to multiple organs in primary lung adenocarcinoma. Metastatic subpopulations isolated from independent lymph node-derived lung adenocarcinoma cell lines harbor a hyperactive WNT/TCF pathway. Reduction of TCF activity in these cells attenuates their ability to form brain and bone metastases in mice, independently of effects on tumor growth in the lungs. The WNT/TCF target genes *HOXB9* and *LEF1* are identified as mediators of chemotactic invasion and colony outgrowth. Thus a distinct WNT/TCF signaling program through LEF1 and HOXB9 enhances the competence of lung adenocarcinoma cells to colonize the bones and the brain.

Introduction

Metastasis is an ominous feature of malignant solid tumors and its natural course varies extensively depending on the type of disease. The tissue and cell of origin of the tumor markedly influence the sites and severity of distant metastasis. Depending on the cancer subtype, metastasis may emerge quickly in multiple organs or in particular organs after a protracted latency period. Breast tumors, for example, undergo dissemination from an early stage (Husemann et al., 2008; Klein et al., 1999), but metastasis to bones, lungs, brain, or liver may not manifest until years or decades after the diagnosis and removal of the primary tumor

Contact: Joan Massagué, Box 116, Memorial Sloan-Kettering Cancer Center, 1275 York Avenue, New York, NY 10065 USA, Phone: 646-888-2044 Fax: 646-422-0197, j-massague@ski.mskcc.org.

(Karrison et al., 1999; Schmidt-Kittler et al., 2003). This course suggests that disseminated breast cells normally require further malignant evolution to overtly colonize distant organs. This process gives rise to organ-specific metastatic cell populations, which has prompted the identification of organ-specific metastasis genes and functions (Nguyen et al., 2009).

Metastasis in other types of cancer follows a different course, with rapid spread to multiple organs. A case in point is lung adenocarcinoma, the most common subtype of lung cancer with a high mortality rate (Hoffman et al., 2000). Even if diagnosed at an early stage and surgically removed, lung adenocarcinomas can relapse within months, spreading to the lymph nodes, contra-lateral lung, adrenal glands, the bones, and the brain (Feld et al., 1984; Hess et al., 2006; Martini et al., 1995). Brain metastasis has particularly morbid physical and cognitive consequences (Gaspar, 2004; Gavrilovic and Posner, 2005; Thomas et al., 2000). Lung adenocarcinoma is a principal source of brain metastasis, due in part to the arterial circulation flowing directly from the lungs to the brain, which pulmonary cancer cells can more easily access (Gaspar, 2004; Gavrilovic and Posner, 2005; Thomas et al., 2000).

The genes and mechanisms that mediate lung adenocarcinoma metastasis are largely unknown. However, the natural course of this disease suggests the acquisition of mechanisms in lung adenocarcinoma cells that allow the aggressive infiltration and colonization of multiple organs soon after cancer cell dispersion from a primary tumor. This hypothesis led us to consider the involvement of developmental pathways as providers of these functions. By combining genome wide transcriptional analysis and experimental modeling, we identified the activation of the WNT/TCF pathway as a determinant of lung adenocarcinoma metastatic competence to multiple organ sites.

The WNT signaling pathway plays major roles in stem cell biology, organogenesis, tissue homeostasis, and cancer (Clevers, 2006; Klaus and Birchmeier, 2008; Logan and Nusse, 2004; Moon et al., 2004). Binding of secreted Wnt ligands to Frizzled and LRP5/6 transmembrane receptors prevents the phosphorylation-dependent polyubiquitination and degradation of the signaling pool of β-catenin in the cytoplasm. This degradation is initiated by a protein complex including APC (the *adenomatous polyposis coli* gene product), Axin, and glycogen synthase kinase-3β (GSK-3β) (Clevers, 2006; Logan and Nusse, 2004). Spared from degradation, β-catenin accumulates in the nucleus and binds to transcription factors of the LEF/TCF (lymphoid enhancer-binding factor and T cell factor) family to regulate gene expression (Arce et al., 2006).

Mutations that constitutively activate the WNT pathway are frequently involved in colorectal cancer initiation (Clevers, 2006; Moon et al., 2004; Morin et al., 1997; Polakis, 2007). However, such mutations are infrequent in lung adenocarcinomas (Ding et al., 2008). Prominent tumor-initiating events in lung adenocarcinoma include KRAS and EGFR mutations (Rodenhuis et al., 1988; Sharma et al., 2007). Surprisingly, we found that gene-expression signatures denoting WNT/TCF pathway activity in lung adenocarcinomas are associated with a high rate of relapse to distant sites. In vivo selection of metastatic cells from independent human lung adenocarcinoma lines yields derivatives that harbor a hyperactive WNT/TCF pathway, in association with an enhanced ability to infiltrate and colonize the brain and bones. Using these cells as a model, we provide functional evidence for the involvement of two WNT target genes, the transcription factors HOXB9 and LEF1, as mediators of chemotactic invasion and colony outgrowth.

Results

A TCF transcriptional signature is associated with lung adenocarcinoma relapse

Because of the propensity of lung adenocarcinomas to rapidly metastasize to multiple organs, and the lack of mutations associated with this transition thus far, we undertook the approach of analyzing a clinical cohort of lung adenocarcinomas using gene-expression signatures that denote activation of specific pathways. We utilized gene sets that were responsive to a K-Ras mutation in a mouse model (Sweet-Cordero et al., 2005), to a dominant-negative TCF4 (dnTCF4) in colon cancer cells (van de Wetering et al., 2002), to treatment of epithelial cells with TGF-β (Padua et al., 2008) or to overexpression of c-Myc, SRC, or E2F3 in human mammary epithelial cells (Bild et al., 2006). We queried gene-expression data on 107 annotated primary lung adenocarcinomas including 65 stage I tumors from patients who had relapsed and who remained disease free (MSKCC set 1, Supplementary Table 1). In an unsupervised analysis, the TCF4 gene signature identified a distinct sub-group (Figure 1A) with an elevated rate of recurrence to multiple organs (Figure 1B, p=0.006). The K-Ras, SRC, and E2F3 signatures were not predictive of increased overall metastasis (Figure 1C). The TGF-β signature, which is associated with lung relapse in estrogen receptor-negative breast tumors (Padua et al., 2008) was not specifically associated with lung adenocarcinoma metastasis, whereas the MYC signature was modestly predictive (Figure 1C, p=0.03). A β-catenin gene set (Bild et al., 2006) was not associated with relapse (data not shown). This set however largely consists of down-regulated genes in the absence of Wnt signal, potentially reflecting β-catenin functions that are independent of TCF transcription (Gottardi and Gumbiner, 2004). Following statistical correction for multiple comparisons, the TCF4 gene set was the only significant predictor of relapse (Bonferroni correction, p=0.042). Because TCF4 is a member of the LEF/TCF family of WNT pathway transcriptional effectors (Arce et al., 2006), we postulated that canonical WNT transcriptional activity may distinguish a subset of lung adenocarcinomas with high competence for metastasis.

An experimental model of lung adenocarcinoma metastasis

To develop an experimental model for the analysis of lung adenocarcinoma metastasis we isolated metastatic subpopulations from two human lung cancer cell lines. The H2030 cell line was established from a lymph node of a stage-III lung adenocarcinoma patient and harbors a *KRAS*^{G12C} mutation (Phelps et al., 1996). The PC9 line was established from a lymph node of a lung adenocarcinoma patient with an *EGFR*$^{\Delta exon19}$ mutation (Koizumi et al., 2005; Sasaki et al., 1991). As these two cell lines were derived from lymph nodes, they provided appropriate systems for the isolation of malignant cells that might harbor multi-organ metastatic competence before adaptation to grow in distant organs.

When placed in the arterial circulation of immunodeficient mice by intracardiac inoculation, both cell lines colonized the bones and brain. We extracted tumor cells from the brain and expanded them in culture for two more rounds of *in vivo* selection (Figure 2A). The resulting BrM3 cell populations consistently demonstrated enriched metastatic activity, as detected by bioluminescence imaging (BLI) and magnetic resonance of the brain or X-ray imaging of the bones (Figure 2B). H2030-BrM3 and PC9-BrM3 cells formed brain metastasis in 100% of animals compared to a 10%-13% efficiency of the parental lines (Figure 2C,D). Although isolated from the brain, the H2030-BrM3 cells and, to a lesser extent, the PC9-BrM3 cells showed an increased ability to colonize the vertebral and limb bones over their starting metastatic potential (Figure 2D). Thus the ability to metastasize to bone and brain are linked in the BrM3 derivatives.

In the bones, PC9-BrM3 and H2030-BrM3 formed osteolytic lesions (Figure 2E,F). PC9-BrM3 and H2030-BrM3 cells avidly colonized the cerebrum and cerebellum, forming nodules as well

as smaller invasive lesions with occasional spread into the meninges (Figure 2G and Supplemental Figure 1A). Invasive metastases in the brain were not angiogenic, but displayed perivascular localization and proliferation (Figure 2H), with gliosis (Figure 2I) and astrocyte proliferation at the invasive edge of metastasis (Supplementary Figure 1B). Importantly, H2030-BrM3 cells implanted orthotopically in the lung could disseminate to the brain independently of lung and pleural tumor burden (Figure 2J).

BrM3 cells did not proliferate faster than their parental populations in monolayer culture, nor were they more resistant to growth factor depletion (Supplementary Figure 2A,B). When implanted with extracellular matrix Matrigel directly into the lungs, H2030-BrM3 cells had an initial growth advantage (Figure 2K, left), whereas PC9-BrM3 cells did not have altered tumorigenic rates compared to their parental counterparts (Figure 2K, right). Similar results were obtained from subcutaneously implanted tumors (data not show). The advantage of H2030-BrM3 cells is consistent with their enhanced colony-forming ability in Matrigel (see below). However, the rate of subsequent expansion of H2030-BrM3 tumors in the lung over 7 weeks was not significantly different from those of the parental line (Figure 2K, left). In sum, these two lung adenocarcinoma models recapitulate salient features of metastasis from lung adenocarcinoma, including the capacity to rapidly disseminate and colonize bone and brain.

Deregulated WNT/TCF activity in highly metastatic lung adenocarcinoma cells

We analyzed the transcriptome of the parental and BrM3 derivatives under basal cell culture conditions. The PC9-BrM3 transcriptome was significantly enriched for the TCF4 classifier and the H2030-BrM3 cells showed a detectable albeit not statistically significant enrichment (Figure 3A). To evaluate the activity of WNT/TCF pathway in these cell lines we performed transcriptional reporter assays using the TOP/FOP reporter system (Korinek et al., 1997). The BrM3 cells in both systems showed higher basal TCF transcriptional activity (2-fold and 2.8-fold, respectively) compared to the corresponding parental lines (Figure 3B). Furthermore, addition of the ligand Wnt3A caused a strong increase in TCF activity in the BrM3 sub-populations, which significantly surpassed the Wnt3a-induced increase in the parental lines (Figure 3B). These results revealed the presence of a deregulated TCF pathway in both metastatic cell populations.

β-catenin is distributed as an abundant membrane associated pool and a free labile pool available for WNT/TCF signaling. The stabilization and nuclear localization of this free pool are necessary for β-catenin as a co-activator of TCF-dependent transcription (Clevers, 2006; Klaus and Birchmeier, 2008; Logan and Nusse, 2004; Moon et al., 2004). Immunoblotting analysis revealed nuclear accumulation of β-catenin following Wnt3a treatment in all adenocarcinoma lines (Figure 3C). Notably, both the cytosolic and nuclear/signaling levels of β-catenin were higher in BrM3 cells compared to parental H2030 cells (Figure 3C). Phosphorylation of β-catenin at Ser33/37 and Thr41 marks the signaling pool for proteosomal degradation (Clevers, 2006). Upon Wnt3A stimulation, β-catenin was more rapidly dephosphorylated at Ser33/37 and Thr41 in H2030-BrM3 cells, indicating a greater rate of stabilization (Figure 3D). In the PC9 derivatives, β-catenin was abundant in both parental and BrM3 cells, suggesting the pre-existence of a hyperactive WNT pathway (Figure 3C). Dephosphoryation of Ser33/37 and Thr41 in response to Wnt3a was similar in the parental and BrM3 PC9 lines, suggesting that enhanced TCF activity in PC9-BrM3 cells may depend on additional alterations (Figure 3D).

Somatic mutations in *APC* or the β-catenin gene *(CTNNB1)* can increase β-catenin stability and activity in colorectal cancer (Clevers, 2006; Moon et al., 2004; Morin et al., 1997; Polakis, 2007). Mutations in these genes have been detected at low frequency in lung adenocarcinomas (Ding et al., 2008). In BrM3 and parental sets, we sequenced *APC*, *CTNNB1* and 13 additional genes (*APC2*, *AXIN1*, *AXIN2*, *GSK3B*, *STK11*, *LEF1*, *TCF7/TCF1*, *TCF7L1/TCF3*, *TCF7L2/*

TCF4, *FRZB*, *SFRP1*, *SFRP2* and *SFRP4*) that encode proximal components of the WNT pathway. No mutations were found to be specifically associated with BrM3 populations, except for a silent mutation in *SFRP4* (G to A, Chromosome 7: 37918251) in H2030-BrM3 cells. qRT-PCR and GeneChip array analysis of 84 WNT pathway related genes (including those sequenced) revealed a common up-regulation of *LEF1* in highly metastatic cells (Figure 3E,F) but no consistent alterations in the expression of any of the other genes (data not shown). These results suggest that hyperactivation of WNT/TCF in these highly metastatic cells is not associated with mutations in core components of the WNT pathway but to other alterations that commonly converge on WNT transcriptional effectors.

A lung adenocarcinoma WNT gene response signature associated with metastasis

Because the TCF4 signature was obtained from a colon cancer cell line (van de Wetering et al., 2002) we asked whether the metastatic potential of lung adenocarcinomas also correlates with a WNT gene-expression response derived specifically from lung adenocarcinoma cells. We generated transcriptomic gene sets from Wnt3a-treated versus untreated cells in both the H2030 and PC9 systems, combining the responses in both parental and metastatic derivatives. To obtain a more comprehensive transcriptional readout, we employed approaches based on a correlation coefficient method (Chang et al., 2005; Saal et al., 2007; Xu et al., 2008). With this method, the expression trends of many pathway-associated genes can be converted into a continuous score that avoids arbitrary expression level criteria and is applicable across multiple data sets.

When tested in our 107-tumor lung adenocarcinoma cohort, the resulting H2030 and PC9 WNT-responsive gene sets were independently associated with metastatic recurrence to multiple organ sites (Supplementary Figure 3A,B). PC9 and H2030 cells express WNT responsive genes which only partial overlap. These differences may reflect pathway activation in the context of different tumor developmental histories. To derive a broader WNT/TCF pathway classifier from these two gene sets, we combined probe sets that were regulated by Wnt3a in at least one experimental system with similar expression trends in the other and which were still associated with clinical outcome in MSKCC set 1 (refer to Experimental Procedures). This yielded a lung cancer WNT gene set (LWS), consisting of 91 probes sets including 81 known genes (Supplementary Table 2).

The LWS displayed improved prediction of metastatic relapse compared to the TCF4 classifier in the initial cohort of primary lung adenocarcinomas (MSKCC set 1, p=0.001; Figure 4A) and notably, in an independent lung adenocarcinoma data set (MSKCC set 2, $p=9.6\times10^{-5}$; Figure 4A) and among lung adenocarcinomas in a cohort of mixed lung tumors (SMC set, p=0.0025; Figure 4B). Importantly, the LWS was associated with recurrence in stage I lung adenocarcinomas (Figure 4C), and did not predict metastasis in squamous lung carcinomas (Figure 4B), or in breast carcinomas (Padua et al., 2008) (Figure 4D). Consistent with our model systems, the LWS predicted distant lung adenocarcinoma relapse to both brain and bone (Supplementary Figure 3C,D). Although the H2030-BrM3 or PC9-BrM3 were brain isolates, we were unable to obtain from these cells a common signature that would predict brain relapse using methods that previously revealed organ-specific metastasis signatures (Minn et al., 2005a). To determine the association of LWS status with overall patient survival we tested four independent stage I lung adenocarcinoma cohorts from a multi-institutional study (Shedden et al., 2008). In three out of the four cohorts tested, the LWS predicted poor survival in stage I adenocarcinomas (Supplementary Figure 4A-E). Altogether these results validate the association of WNT hyperactivation with distant multi-organ metastatic potential of lung adenocarcinomas.

By using the LWS in a Pearson correlation coefficient score, we compared brain samples from lung adenocarcinoma patients (n=28; Figure 4E) to either primary lung adenocarcinomas from

patients who remained disease-free over 5 years (n=53) or primary lung adenocarcinomas from patients who recurred in any site (n=43). Lung adenocarcinoma metastases to bone are rarely resected, and were not available for study. The expression trends of LWS genes in brain metastases resembled more closely primary adenocarcinomas that recurred (Figure 4E). Thus, the activation of WNT/TCF appears to be maintained during brain metastatic progression in clinical samples.

LEF1 and *HOXB9* are WNT/TCF targets that mediate metastasis

To evaluate the functional role of WNT/TCF signaling in lung adenocarcinoma metastasis, we disrupted this pathway by expressing dominant negative TCFs (dnTCF1 and/or dnTCF4) that lack the n-terminal binding site for β-catenin (van de Wetering et al., 2002). Stable expression of dnTCF4 in H2030-BrM3 cells partially decreased the TCF activity (Supplementary Figure 5A,B) and metastatic activity of these cells (Figure 5A). Co-expression of dnTCF1 and dnTCF4 in PC9-BrM3 cells (Supplementary Figure 5C,D) abated the metastatic activity of these cells in different organs in the same mouse (Figure 5B). This reduction in TCF activity had little effect on BrM3 pulmonary growth (Figure 5C,D).

To identify mediators of WNT pro-metastatic functions, we focused on a subset of LWS genes whose expression level was strongly correlated with the metastatic potential of our cell derivatives and are implicated in developmental programs. Three genes that fulfilled these criteria were *lymphoid enhancer-binding factor 1* (*LEF1*), *homeobox B9* (*HOXB9*), and *bone morphogenetic protein 4* (*BMP4*). *HOXB9* is a TCF4 target (Hatzis et al., 2008) and belongs to the homeobox transcription factor gene family, which is critical for embryonic segmentation and limb patterning (Abate-Shen, 2002). *LEF1* encodes a transcriptional effector of the canonical WNT pathway in addition to being a target of Wnt3a and TCF4. LEF1 upregulation by WNT may mediate signal amplification during malignancy (Hovanes et al., 2001). *BMP4* belongs to the TGF-β superfamily, can be induced by WNT and regulates stem cell differentiation and multiple developmental processes (Shu et al., 2005; ten Dijke et al., 2003; Varga and Wrana, 2005).

The expression level of *LEF1* and *HOXB9* was marginal in parental H2030 cells, but was increased and potently induced by Wnt3a in the H2030-BrM3 cells (Figure 5E). In parental PC9 cells, Wnt3a addition augmented the expression level of *LEF1* and *HOXB9*, whereas these genes were highly expressed and no further inducible by Wnt3a in PC9-BrM3 cells (Figure 5E). Expression of dnTCFs decreased the expression of *LEF1* and *HOXB9* to Wnt3a in BrM3 cells (Figure 5F). Thus the response patterns of *LEF1* and *HOXB9* are consistent with a constitutive hyperactivation of WNT/TCF signaling in PC9 cells (refer to Figure 3 C,D) and a hypersensitivity to Wnt stimulation in H2030 cells.

To achieve more specific inhibition of putative WNT/TCF pro-metastatic genes, we decreased *LEF1* or *HOXB9* by stable RNAi-mediated knockdown in BrM3 derivatives (Supplementary Figure 6A). Knockdown of *LEF1* or *HOXB9* significantly decreased the ability of H2030-BrM3 and PC9-BrM3 cells to form bone and brain metastases (Figure 6A and Supplementary Figure 6B). Knockdown of *BMP4* had no effect on metastasis (data not shown). Reduction of *LEF1* or *HOXB9* did not affect the growth of PC9-BrM3 cells implanted in the lung (Supplementary Figure 7A). In H2030-BrM3 cells, *HOXB9* knockdown did not affect lung and pleural growth rates whereas *LEF1* knockdown had a partial inhibitory effect (Supplementary Figure 7B). These results are consistent with the tumor reinitiating advantage of H2030-BrM3 but not PC9-BrM3 cells over their parental counterparts in the lungs (refer to Supplementary Figure 2D). Moreover, overexpression of *LEF1* and *HOXB9* in the parental H2030 and PC9 cell lines increased their metastatic activity from circulation to bone and brain (Supplementary Figure 8 and Figure 6B-E). Collectively these results suggest that *HOXB9* and *LEF1* can enhance the competence of lung adenocarcinoma for brain and bone metastasis.

LEF1 and HOXB9 as mediators of colony outgrowth and chemotactic cell invasion

The biological properties of LEF1 and HOXB9 were further studied *ex-vivo* using the H2030-BrM3 population, which has a low threshold for exogenous WNT activation. Given the link between WNT/TCF and metastasis to multiple organs, we focused on the general functions of metastatic outgrowth and invasion. Knockdown of LEF1 and HOXB9 did not affect general cell viability in monolayer culture (Supplementary Figure 2A-B). However, when cultured in Matrigel, H2030-BrM3 cells formed compact spherical colonies that grew larger in size (Figure 7A) and in number compared to the parental H2030 cells (Figure 7B, black bars). Wnt3a addition further increased the colony outgrowth (Figure 7B, yellow bars), consistent with the tumor re-initiation advantage of these cells when implanted in the lung. Interestingly, knockdown of *LEF1* expression decreased the size (Figure 7A) and number of the metastatic H2030-BrM3 colonies (Figure 7B), whereas decreasing *HOXB9* expression had no effect.

To analyze metastatic invasion, we measured the infiltration of these cells through Matrigel in a modified Boyden chamber assay (Figure 7C). Parental H2030 and H2030-BrM3 cells showed a similar basal ability to infiltrate Matrigel (Figure 7D). However, given the strong astrocytic reaction elicited at the invasive edge of metastatic lesions in vivo (refer to Figure 2I) we repeated the invasion assays using astrocyte-conditioned media as a source of chemoattractant in the bottom chamber. Under these conditions, the invasive activity of H2030-BrM3 was significantly higher than that of parental cells (Figure 7D). Pre-incubation of H2030-BrM3 cells with Wnt3a increased their invasion towards stromal conditioned media (Figure 7D, blue bars). Wnt3A stimulated the invasion of the parental PC9 cells, while PC9-BrM3 cell displayed higher basal invasiveness (Supplementary Figure 9) consistent with their expression of *LEF1* and *HOXB9*. Wnt3a did not act as a chemoatractant, since invasion was unaffected by the addition of Wnt3a to the bottom chamber (data not shown). Notably, shRNA-mediated knockdown of either *LEF1* or *HOXB9* inhibited invasion in H2030-BrM3 as well as PC9-BrM3 cells (Figure 7E). The metastatic potential of BrM3 cells and their Wnt3A responsiveness were not associated with changes in the TCF target *c-myc*, nor were these phenotypes linked to markers of epithelial-mesenchymal transition, such as loss of E-cadherin or gain of vimentin expression (Supplementary Figure 10).

Discussion

The evidence presented here suggests that a hyperactive WNT/TCF pathway enhances the ability of human lung adenocarcinomas to develop brain and bone metastases. Two WNT target genes, *LEF1* and *HOXB9*, are identified as promoters of lung adenocarcinoma metastasis and mediators of chemotactic invasion and colony outgrowth. These findings provide insights into the determinants of the typically rapid, multi-organ metastatic progression of this disease.

WNT/TCF signaling mediates lung adenocarcinoma metastasis

We have generated a lung cancer WNT gene response set –the LWS– that identifies lung adenocarcinomas with aggressive biological characteristics and poor clinical outcome. WNT/TCF pathway activation as detected by gene expression is associated with metastasis to brain and bones, two prominent sites of distant relapse in lung adenocarcinoma. The LWS can distinguish early stage I lung adenocarcinomas from independent cohorts of patients that are most likely to progress. However, it does not predict relapse in squamous lung carcinoma or breast carcinoma. The transcriptional output of WNT activation is context-dependent (Clevers, 2006; Logan and Nusse, 2004) and we do not exclude the possibility that other WNT targets or different pathway combinations may also contribute to lung cancer progression. Nevertheless, our evidence indicates a unique association between the WNT/TCF pathway and metastatic propensity in human lung adenocarcinomas.

Hyperactivation of WNT/TCF is a uniform property of highly metastatic subpopulations that we obtained from different human lung adenocarcinoma cell lines. These cells lines correspond to two distinct and defined subtypes of lung adenocarcinoma –the EGFR and KRAS molecular subtypes. *KRAS* and *EGFR* mutations are present in approximately 25% and 20% of human lung adenocarcinomas respectively (Rodenhuis et al., 1988; Sharma et al., 2007), and have been validated as oncogenes. However, lung adenocarcinomas initiated by these mutations require additional alterations in order to metastasize to distant sites (Ji et al., 2006; Johnson et al., 2001; Politi et al., 2006). The fact that these cell lines were derived from lymph node samples suggests that the acquisition of a hyperactive WNT/TCF pathway within a subset of malignant cells preceded their colonization of distant organs.

The hyperactivation of WNT/TCF in our model of metastatic lung adenocarcinomas does not correlate with a preponderance of typical somatic mutations in this pathway. Mutations in WNT pathway components are common tumor-initiating events in colorectal and gastric cancers but are less frequent in lung adenocarcinomas (Ding et al., 2008). Deregulation of this pathway may result from additional epigenetic alterations. Interestingly, *APC* methylation has been noted in metastatic non-small cell lung cancers (Brock et al., 2008). While the diverse mechanisms that regulate the WNT pathway in our models remain to be elucidated, an end result of this process is the elevated expression of at least two transcription factors, *LEF1* and *HOXB9* that encode different pro-metastatic functions, some of which are not required for tumor growth in the lung. The activation in primary tumors of pro-metastatic functions that provide no local growth advantage is not without precedent (Karnoub et al., 2007; Padua et al., 2008). The hyperactivity of the WNT/TCF pathway in lung adenocarcinomas observed here might reflect a presence of Wnt ligands in the tumor stroma, a feature of the tumor cell of origin, an epigenetic bystander alteration of WNT/TCF pathway components, or a combination of these mechanisms.

LEF1 and HOXB9 are effectors of the WNT metastasis program

LEF1 and *HOXB9* are direct transcriptional targets of the TCF4 transcription factor (Hatzis et al., 2008). HOXB9 is part of a homeobox family gene cluster whose expression is normally restricted to embryogenesis (Abate-Shen, 2002). HOXB9 expression has been reported in lung cancer cell lines (Calvo et al., 2000), but its function is unknown. LEF1 is a prototypical transcriptional mediator of WNT gene response, and its activation may amplify pathological WNT signaling (Hovanes et al., 2001). Moreover, LEF1 can interact with co-factors independently of β-catenin that cooperate in WNT transcriptional responses (Arce et al., 2006). High basal levels of *LEF1* in metastatic cells may increase transcriptional responses without additional changes in β-catenin.

In our lung adenocarcinoma model, WNT/TCF hyperactivation can stimulate bone and brain metastasis independently of changes in intrinsic tumor cell proliferation or of a general growth advantage. We show that HOXB9 and LEF1 increase cancer cell invasion and LEF1 promotes tumor colony outgrowth in extracellular matrix. Interestingly, the phenotype of our metastatic derivatives resembles that described for bronchioalveolar stem cells (BASCs) with reduced differentiation and increased self-renewal properties (Kim et al., 2005). BASCs exhibit enhanced WNT activity following injury (Zhang et al., 2008). Thus HOXB9 and LEF1 may fulfill progenitor cell functions that are re-enacted during metastatic progression. The stem cell reprogramming gene c-*MYC* is a target of the LEF/TCF pathway in colon cancer cells (He et al., 1998) but not in the lund adenocarcinoma lines studied here. However, we do not exclude the possible involvement of other WNT target genes in lung adenocarcinoma metastasis.

Early metastatic competence versus progressive metastatic speciation

The present findings illuminate a central concept in lung adenocarcinoma progression, namely, the role of a pro-metastatic signal that is acquired in primary tumors and enables their rapid metastatic spread. Unlike breast or prostate cancer metastasis, which may develop years to decades after the removal of a primary tumor, lung adenocarcinomas are typically competent to metastasize rapidly to multiple organs. The long latency of metastasis in breast or prostate carcinoma implies the need for further malignant evolution of the disseminated cancer cells in the infiltrated organs. In contrast to the protracted evolution of cancers which undergo long periods of remission before clinical metastasis, the short latency of relapse in lung adenocarcinomas predicts their acquisition of a pro-metastatic program early on and a lesser degree of organ speciation. Our identification of a mechanism that provides overall metastatic competence in early stage lung adenocarcinomas is in agreement with these predictions.

Intra-cranial relapses are a significant source of failure following treatments with chemotherapy (Chen et al., 2007) and targeted drugs (Omuro et al., 2005). While animal models of lung cancer represent a critical venue to address this problem, genetically modified mouse models of lung cancer reported to date yield metastatic tumors that occur in visceral organs but not in the brain (Jackson et al., 2005; Zheng et al., 2007). While not without limitations, our experimental systems recapitulate important phenotypic and molecular features of lung adenocarcinoma, including brain and bone metastasis, and a hyperactive WNT/TCF pathway in the background of relevant oncogenic mutations. This model may be useful for achieving a deeper understanding of early metastatic events and the development of improved treatments for lung adenocarcinoma patients at risk for metastasis.

Experimental Procedures

Additional methods for cell culture, in vivo selection, in vitro assays, immunostaining procedures, retroviral shRNA targets, sequencing, and gene expression analysis are provided in a Supplemental Section.

Animal Studies

Animal procedures were in accordance with the MSKCC Institutional Animal Care and Use Committee. Xenograft were performed on mice with SCID mutation in a nonobese diabetic background (NOD.SCID), or mice carrying the nude mutation crossed to the CBA/N X-chromosome-linked immune defect and beige mutations (bg-nu-Xid). Animals were aged-matched between 4-6 weeks. NSCLC cell lines were engineered to stably express a triple modality vector encoding *GFP-luciferase* fusion (Minn et al., 2005b). For experimental metastasis assays, between 10^4 and 10^5 cells were re-suspended in 0.1 mL PBS and injected into the right ventricle. Metastasis was detected by bioluminescence using an IVIS 200 Xenogen and confirmed by X-ray, MRI, and/or histology. Incidence of metastasis was quantified based on the luminescent signal in limbs and/or brain at a given time point and presented as Kaplan-Meir curves. For lung tumorigenesis, 10^4 cells were re-suspended in a 1:2 mixture of PBS and growth factor reduced Matrigel (BD Biosciences), and injected into the lung through the left rib cage of mice as previously described (Doki et al., 1999). Alternatively, cells were injected into the lateral tail vein. Growth rate in the lung/pleura was measured as a function of lung photon flux normalized to day 0 in live animals. Tumorigenic growth rates were similar when implanted subcutaneously. Metastasis phenotype was independent of animal sex.

LEF/TCF reporter assays

The TOP-Flash and FOP-Flash promoters were subcloned into pGL4.82-Renilla luciferase constructs (Promega). Cells were transfected using Lipofectamine 2000 and selected for two

days in puromicin. Transfected cell were then re-seeded into 24 well plates at 50,000 cells/well before treatment with recombinant Wnt3a (50 -100ng/ml; R&D Systems) for 12 hours. Reporter assays were performed according to the manufacturer's instructions (Promega). Promoter activity was calculated as the ratio of specific TOP-Flash over non-specific FOP-Flash relative renilla luciferase units (RLU).

Gene expression profiling

Subconfluent parental and metastatic derivatives were serum starved overnight, and either mock treated or stimulated with recombinant Wnt3A (75-100ng/ml) for 3 hours. RNA was extracted from duplicate samples of each condition using the RNeasy mini kit (Qiagen). Labeling and hybridization of the cell line samples to the HG-U133A_2 gene expression chip (Affymetrix) was performed by the MSKCC Genomics Core Facility. Microarray data from a cohort of 107 lung adenocarcinoma tumors (MSKCC set 1), a second cohort of 129 adenocarcinomas (MSKCC set 2) including tumors from Chitale al. (Chitale et al., 2009) as well as 28 brain metastasis, were analyzed on Affymetrix HG-U133A and HG-U133A_2 platforms. A third data set containing a mix of lung adenocarcinomas and squamous carcinomas from the Samsung Medical Center (SMC set; HG-U133A Plus 2.0) was publicly available. For pathway and correlation coefficient analysis, raw CEL data were preprocessed using RMA algorithm implemented by the *affy* package of *R* statistical software (designated as *R* hereafter). Gene expression data of cell derivatives is deposited at GEO (GSE14107). Samsung Medical Center set was obtained from GEO (GSE8894). Raw data and clinical annotation for MSKCC sets 1, 2, and brain metastasis are available at http://cbio.mskcc.org/Public/lung_array_data/.

Pathway signature derivation

Genes regulated by KRAS and dnTCF4 were extracted from published results (Sweet-Cordero et al., 2005; van de Wetering et al., 2002) and matched to the corresponding Affymetrix probes (HG-U133A platform). The Affymetrix version of the TCF4 signature was used to cluster MSKCC set 1 in an unsupervised manner (by the "*heatmap.2*" function of "*gplots*" package of *R*). The cluster that overexpresses the majority of dnTCF4 genes was defined as TCF4+, and the other cluster was defined as TCF4-. The clinical outcomes of the two clusters were compared by log-rank test using the "*survdiff*" function of "*survival*" package of *R*. β-catenin, c-myc, SRC, E2F3, and TGF-β gene lists were obtained from previous results (Bild et al., 2006; Padua et al., 2008) and used for unsupervised analysis.

Derivation and characterization of the LWS

A combinatory approach based on correlation coefficient score and unsupervised clustering was used to evaluate the association between Wnt3A mediated transcriptional activation in lung adenocarincoma cell lines and relapse in MSKCC sets 1, 2, and SMC lung adenocarcinoma clinical cohorts. This was confirmed using pathway meta-analysis. A comprehensive description of these methods and the derivation of the Lung cancer WNT responsive gene set (LWS) are provided in supplementary material.

Supplementary Material

Refer to Web version on PubMed Central for supplementary material.

Acknowledgments

We would like to express deep gratitude to our late colleague William L. Gerald. We are indebted to H. Varmus, W. Pao, V. Rusch, and members of the Massagué laboratory for insightful discussions. We thank A. Heguy for supervising sequencing and mutational analysis. H. Clevers, E. Batlle, R. Moon, W. Pao, and H. Varmus generously provided constructs and cell lines. This work was supported by National Institutes of Health grant P01-129243 (M.G.K., M.L.,

W.L.G., and J.M.). DXN was the Bayer postdoctoral fellow of the Damon Runyon Cancer Research Foundation. ACC was supported by an ASCO CDA grant. JM is an Investigator of the Howard Hughes Medical Institute.

References

Abate-Shen C. Deregulated homeobox gene expression in cancer: cause or consequence? Nat Rev Cancer 2002;2:777–785. [PubMed: 12360280]

Arce L, Yokoyama NN, Waterman ML. Diversity of LEF/TCF action in development and disease. Oncogene 2006;25:7492–7504. [PubMed: 17143293]

Bild AH, Yao G, Chang JT, Wang Q, Potti A, Chasse D, Joshi MB, Harpole D, Lancaster JM, Berchuck A, et al. Oncogenic pathway signatures in human cancers as a guide to targeted therapies. Nature 2006;439:353–357. [PubMed: 16273092]

Brock MV, Hooker CM, Ota-Machida E, Han Y, Guo M, Ames S, Glockner S, Piantadosi S, Gabrielson E, Pridham G, et al. DNA methylation markers and early recurrence in stage I lung cancer. N Engl J Med 2008;358:1118–1128. [PubMed: 18337602]

Calvo R, West J, Franklin W, Erickson P, Bemis L, Li E, Helfrich B, Bunn P, Roche J, Brambilla E, et al. Altered HOX and WNT7A expression in human lung cancer. Proc Natl Acad Sci U S A 2000;97:12776–12781. [PubMed: 11070089]

Chang HY, Nuyten DS, Sneddon JB, Hastie T, Tibshirani R, Sorlie T, Dai H, He YD, van't Veer LJ, Bartelink H, et al. Robustness, scalability, and integration of a wound-response gene expression signature in predicting breast cancer survival. Proc Natl Acad Sci U S A 2005;102:3738–3743. [PubMed: 15701700]

Chen AM, Jahan TM, Jablons DM, Garcia J, Larson DA. Risk of cerebral metastases and neurological death after pathological complete response to neoadjuvant therapy for locally advanced nonsmall-cell lung cancer: clinical implications for the subsequent management of the brain. Cancer 2007;109:1668–1675. [PubMed: 17342770]

Chitale D, Gong Y, Taylor B, Broderick S, Brennan C, Somwar R, Golas B, Wang L, Motoi N, Szoke J, et al. An integrated genomic analysis of lung cancer reveals loss of DUSP4 in EGFR-mutant tumors. Oncogene. 2009in press

Clevers H. Wnt/beta-catenin signaling in development and disease. Cell 2006;127:469–480. [PubMed: 17081971]

Ding L, Getz G, Wheeler DA, Mardis ER, McLellan MD, Cibulskis K, Sougnez C, Greulich H, Muzny DM, Morgan MB, et al. Somatic mutations affect key pathways in lung adenocarcinoma. Nature 2008;455:1069–1075. [PubMed: 18948947]

Doki Y, Murakami K, Yamaura T, Sugiyama S, Misaki T, Saiki I. Mediastinal lymph node metastasis model by orthotopic intrapulmonary implantation of Lewis lung carcinoma cells in mice. Br J Cancer 1999;79:1121–1126. [PubMed: 10098745]

Feld R, Rubinstein LV, Weisenberger TH. Sites of recurrence in resected stage I non-small-cell lung cancer: a guide for future studies. J Clin Oncol 1984;2:1352–1358. [PubMed: 6512581]

Gaspar LE. Brain metastases in lung cancer. Expert Rev Anticancer Ther 2004;4:259–270. [PubMed: 15056056]

Gavrilovic IT, Posner JB. Brain metastases: epidemiology and pathophysiology. J Neurooncol 2005;75:5–14. [PubMed: 16215811]

Gottardi CJ, Gumbiner BM. Distinct molecular forms of beta-catenin are targeted to adhesive or transcriptional complexes. J Cell Biol 2004;167:339–349. [PubMed: 15492040]

Hatzis P, van der Flier LG, van Driel MA, Guryev V, Nielsen F, Denissov S, Nijman IJ, Koster J, Santo EE, Welboren W, et al. Genome-wide pattern of TCF7L2/TCF4 chromatin occupancy in colorectal cancer cells. Mol Cell Biol 2008;28:2732–2744. [PubMed: 18268006]

He TC, Sparks AB, Rago C, Hermeking H, Zawel L, da Costa LT, Morin PJ, Vogelstein B, Kinzler KW. Identification of c-MYC as a target of the APC pathway. Science 1998;281:1509–1512. [PubMed: 9727977]

Hess KR, Varadhachary GR, Taylor SH, Wei W, Raber MN, Lenzi R, Abbruzzese JL. Metastatic patterns in adenocarcinoma. Cancer 2006;106:1624–1633. [PubMed: 16518827]

Hoffman PC, Mauer AM, Vokes EE. Lung cancer. Lancet 2000;355:479–485. [PubMed: 10841143]

Hovanes K, Li TW, Munguia JE, Truong T, Milovanovic T, Lawrence Marsh J, Holcombe RF, Waterman ML. Beta-catenin-sensitive isoforms of lymphoid enhancer factor-1 are selectively expressed in colon cancer. Nat Genet 2001;28:53–57. [PubMed: 11326276]

Husemann Y, Geigl JB, Schubert F, Musiani P, Meyer M, Burghart E, Forni G, Eils R, Fehm T, Riethmuller G, Klein CA. Systemic spread is an early step in breast cancer. Cancer Cell 2008;13:58–68. [PubMed: 18167340]

Jackson EL, Olive KP, Tuveson DA, Bronson R, Crowley D, Brown M, Jacks T. The differential effects of mutant p53 alleles on advanced murine lung cancer. Cancer Res 2005;65:10280–10288. [PubMed: 16288016]

Ji H, Li D, Chen L, Shimamura T, Kobayashi S, McNamara K, Mahmood U, Mitchell A, Sun Y, Al-Hashem R, et al. The impact of human EGFR kinase domain mutations on lung tumorigenesis and in vivo sensitivity to EGFR-targeted therapies. Cancer Cell 2006;9:485–495. [PubMed: 16730237]

Johnson L, Mercer K, Greenbaum D, Bronson RT, Crowley D, Tuveson DA, Jacks T. Somatic activation of the K-ras oncogene causes early onset lung cancer in mice. Nature 2001;410:1111–1116. [PubMed: 11323676]

Karnoub AE, Dash AB, Vo AP, Sullivan A, Brooks MW, Bell GW, Richardson AL, Polyak K, Tubo R, Weinberg RA. Mesenchymal stem cells within tumour stroma promote breast cancer metastasis. Nature 2007;449:557–563. [PubMed: 17914389]

Karrison TG, Ferguson DJ, Meier P. Dormancy of mammary carcinoma after mastectomy. J Natl Cancer Inst 1999;91:80–85. [PubMed: 9890174]

Kim CF, Jackson EL, Woolfenden AE, Lawrence S, Babar I, Vogel S, Crowley D, Bronson RT, Jacks T. Identification of bronchioalveolar stem cells in normal lung and lung cancer. Cell 2005;121:823–835. [PubMed: 15960971]

Klaus A, Birchmeier W. Wnt signalling and its impact on development and cancer. Nat Rev Cancer 2008;8:387–398. [PubMed: 18432252]

Klein CA, Schmidt-Kittler O, Schardt JA, Pantel K, Speicher MR, Riethmuller G. Comparative genomic hybridization, loss of heterozygosity, and DNA sequence analysis of single cells. Proc Natl Acad Sci U S A 1999;96:4494–4499. [PubMed: 10200290]

Koizumi F, Shimoyama T, Taguchi F, Saijo N, Nishio K. Establishment of a human non-small cell lung cancer cell line resistant to gefitinib. Int J Cancer 2005;116:36–44. [PubMed: 15761868]

Korinek V, Barker N, Morin PJ, van Wichen D, de Weger R, Kinzler KW, Vogelstein B, Clevers H. Constitutive transcriptional activation by a beta-catenin-Tcf complex in APC-/- colon carcinoma. Science 1997;275:1784–1787. [PubMed: 9065401]

Logan CY, Nusse R. The Wnt signaling pathway in development and disease. Annu Rev Cell Dev Biol 2004;20:781–810. [PubMed: 15473860]

Martini N, Bains MS, Burt ME, Zakowski MF, McCormack P, Rusch VW, Ginsberg RJ. Incidence of local recurrence and second primary tumors in resected stage I lung cancer. J Thorac Cardiovasc Surg 1995;109:120–129. [PubMed: 7815787]

Minn AJ, Gupta GP, Siegel PM, Bos PD, Shu W, Giri DD, Viale A, Olshen AB, Gerald WL, Massague J. Genes that mediate breast cancer metastasis to lung. Nature 2005a;436:518–524. [PubMed: 16049480]

Minn AJ, Kang Y, Serganova I, Gupta GP, Giri DD, Doubrovin M, Ponomarev V, Gerald WL, Blasberg R, Massague J. Distinct organ-specific metastatic potential of individual breast cancer cells and primary tumors. J Clin Invest 2005b;115:44–55. [PubMed: 15630443]

Moon RT, Kohn AD, De Ferrari GV, Kaykas A. WNT and beta-catenin signalling: diseases and therapies. Nat Rev Genet 2004;5:691–701. [PubMed: 15372092]

Morin PJ, Sparks AB, Korinek V, Barker N, Clevers H, Vogelstein B, Kinzler KW. Activation of beta-catenin-Tcf signaling in colon cancer by mutations in beta-catenin or APC. Science 1997;275:1787–1790. [PubMed: 9065402]

Nguyen DX, Bos PB, Massaue J. Metastasis: from dissemination to organ-specific colonization. Nat Rev Cancer. 2009in press

Omuro AM, Kris MG, Miller VA, Franceschi E, Shah N, Milton DT, Abrey LE. High incidence of disease recurrence in the brain and leptomeninges in patients with nonsmall cell lung carcinoma after response to gefitinib. Cancer 2005;103:2344–2348. [PubMed: 15844174]

Padua D, Zhang XH, Wang Q, Nadal C, Gerald WL, Gomis RR, Massague J. TGFbeta primes breast tumors for lung metastasis seeding through angiopoietin-like 4. Cell 2008;133:66–77. [PubMed: 18394990]

Phelps RM, Johnson BE, Ihde DC, Gazdar AF, Carbone DP, McClintock PR, Linnoila RI, Matthews MJ, Bunn PA Jr, Carney D, et al. NCI-Navy Medical Oncology Branch cell line data base. J Cell Biochem Suppl 1996;24:32–91. [PubMed: 8806092]

Polakis P. The many ways of Wnt in cancer. Curr Opin Genet Dev 2007;17:45–51. [PubMed: 17208432]

Politi K, Zakowski MF, Fan PD, Schonfeld EA, Pao W, Varmus HE. Lung adenocarcinomas induced in mice by mutant EGF receptors found in human lung cancers respond to a tyrosine kinase inhibitor or to down-regulation of the receptors. Genes Dev 2006;20:1496–1510. [PubMed: 16705038]

Rodenhuis S, Slebos RJ, Boot AJ, Evers SG, Mooi WJ, Wagenaar SS, van Bodegom PC, Bos JL. Incidence and possible clinical significance of K-ras oncogene activation in adenocarcinoma of the human lung. Cancer Res 1988;48:5738–5741. [PubMed: 3048648]

Saal LH, Johansson P, Holm K, Gruvberger-Saal SK, She QB, Maurer M, Koujak S, Ferrando AA, Malmstrom P, Memeo L, et al. Poor prognosis in carcinoma is associated with a gene expression signature of aberrant PTEN tumor suppressor pathway activity. Proc Natl Acad Sci U S A 2007;104:7564–7569. [PubMed: 17452630]

Sasaki Y, Shinkai T, Eguchi K, Tamura T, Ohe Y, Ohmori T, Saijo N. Prediction of the antitumor activity of new platinum analogs based on their ex vivo pharmacodynamics as determined by bioassay. Cancer Chemother Pharmacol 1991;27:263–270. [PubMed: 1847845]

Schmidt-Kittler O, Ragg T, Daskalakis A, Granzow M, Ahr A, Blankenstein TJ, Kaufmann M, Diebold J, Arnholdt H, Muller P, et al. From latent disseminated cells to overt metastasis: genetic analysis of systemic breast cancer progression. Proc Natl Acad Sci U S A 2003;100:7737–7742. [PubMed: 12808139]

Sharma SV, Bell DW, Settleman J, Haber DA. Epidermal growth factor receptor mutations in lung cancer. Nat Rev Cancer 2007;7:169–181. [PubMed: 17318210]

Shedden K, Taylor JM, Enkemann SA, Tsao MS, Yeatman TJ, Gerald WL, Eschrich S, Jurisica I, Giordano TJ, Misek DE, et al. Gene expression-based survival prediction in lung adenocarcinoma: a multi-site, blinded validation study. Nat Med. 2008

Shu W, Guttentag S, Wang Z, Andl T, Ballard P, Lu MM, Piccolo S, Birchmeier W, Whitsett JA, Millar SE, Morrisey EE. Wnt/beta-catenin signaling acts upstream of N-myc, BMP4, and FGF signaling to regulate proximal-distal patterning in the lung. Dev Biol 2005;283:226–239. [PubMed: 15907834]

Sweet-Cordero A, Mukherjee S, Subramanian A, You H, Roix JJ, Ladd-Acosta C, Mesirov J, Golub TR, Jacks T. An oncogenic KRAS2 expression signature identified by cross-species gene-expression analysis. Nat Genet 2005;37:48–55. [PubMed: 15608639]

ten Dijke P, Korchynskyi O, Valdimarsdottir G, Goumans MJ. Controlling cell fate by bone morphogenetic protein receptors. Mol Cell Endocrinol 2003;211:105–113. [PubMed: 14656483]

Thomas AJ, Rock JP, Johnson CC, Weiss L, Jacobsen G, Rosenblum ML. Survival of patients with synchronous brain metastases: an epidemiological study in southeastern Michigan. J Neurosurg 2000;93:927–931. [PubMed: 11117864]

van de Wetering M, Sancho E, Verweij C, de Lau W, Oving I, Hurlstone A, van der Horn K, Batlle E, Coudreuse D, Haramis AP, et al. The beta-catenin/TCF-4 complex imposes a crypt progenitor phenotype on colorectal cancer cells. Cell 2002;111:241–250. [PubMed: 12408868]

Varga AC, Wrana JL. The disparate role of BMP in stem cell biology. Oncogene 2005;24:5713–5721. [PubMed: 16123804]

Xu L, Shen SS, Hoshida Y, Subramanian A, Ross K, Brunet JP, Wagner SN, Ramaswamy S, Mesirov JP, Hynes RO. Gene expression changes in an animal melanoma model correlate with aggressiveness of human melanoma metastases. Mol Cancer Res 2008;6:760–769. [PubMed: 18505921]

Zhang Y, Goss AM, Cohen ED, Kadzik R, Lepore JJ, Muthukumaraswamy K, Yang J, DeMayo FJ, Whitsett JA, Parmacek MS, Morrisey EE. A Gata6-Wnt pathway required for epithelial stem cell development and airway regeneration. Nat Genet 2008;40:862–870. [PubMed: 18536717]

Zheng S, El-Naggar AK, Kim ES, Kurie JM, Lozano G. A genetic mouse model for metastatic lung cancer with gender differences in survival. Oncogene 2007;26:6896–6904. [PubMed: 17486075]

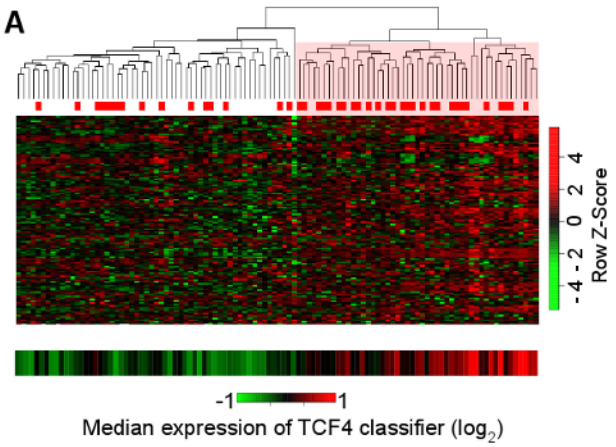

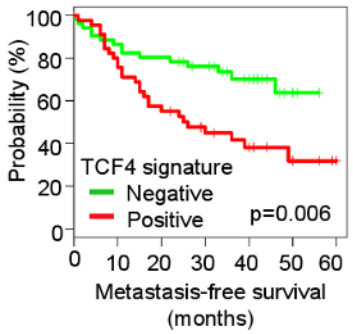

C

Pathway signature	Lung adenocarc. recurrence	Breast cancer recurrence
TGFβ	0.54	0.02
KRAS	0.28	0.35
TCF4	0.006	0.11
SRC	0.193	0.62
E2F3	0.402	(0.04)
MYC	0.03	0.36

Figure 1. A subset of TCF4 target genes associated with lung adenocarcinoma metastasis

(A) Hierarchical clustering of 107 clinically annotated human lung adenocarcinomas (MSKCC set 1) using a list of 73 TCF4 regulated genes available on the U133A Affymetrix chip, segregates a set of tumors (red block) with a high proportion of relapses (red bars). R Value=0.73. Bottom row represents the median expression value of TCF4 target genes. **(B)** Kaplan-Meier curves for metastasis-free survival to all sites according to TCF4 signature. **(C)** Metastasis-free prediction of other pathway classifiers in MSKCC set 1 and a cohort of 368 primary breast tumors. p-value in parentheses denotes inverse correlation. p-values calculated by Log rank test.

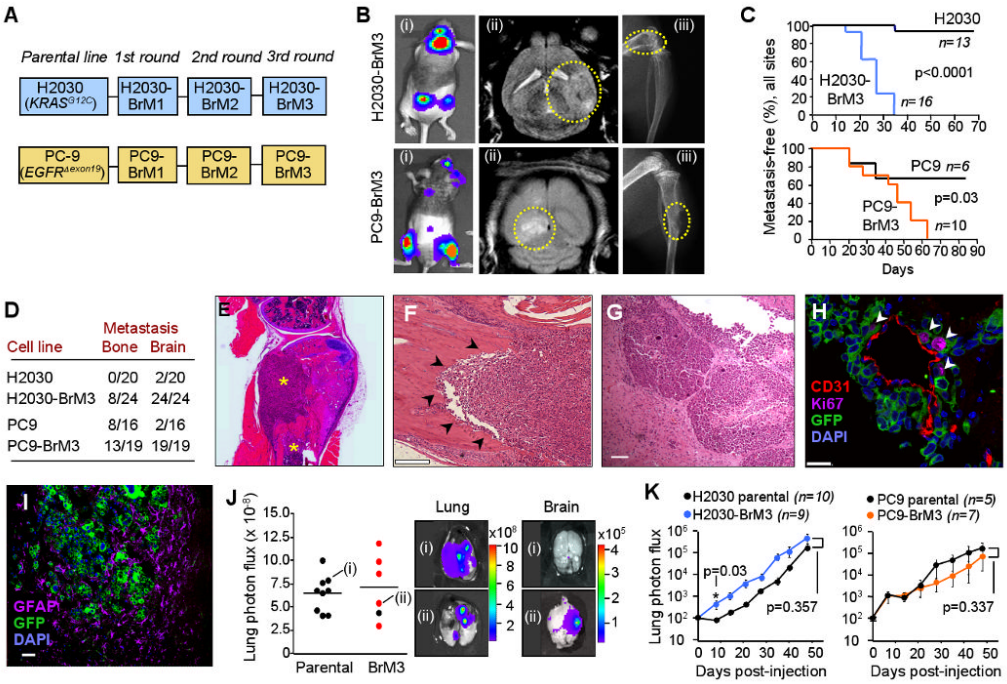

Figure 2. Experimental model of lung adenocarcinoma metastasis

(A) *In vivo* selection scheme for the isolation of metastatic populations (BrM3) from the NCI-H2030 and PC9 lung adenocarcinoma lines. **(B)** Shown are representative bioluminescent images **(i)** of brain, limb and spine metastasis. Brain and bone lesions were confirmed via MRI **(ii)** and X-ray respectively **(iii)**. **(C)** Kaplan-Meier curves of metastasis incidence (brain and/or bone) in mice inoculated with 10^4 cells. Parental H2030 cells versus H2030-BrM3 derivatives (top). PC9 parental versus PC9-BrM3 cells (bottom). p values calculated by Log rank test. **(D)** Frequency and distribution of metastasis following inoculation of 5×10^4 cells. **(E)** Hematoxylin and eosin (H&E) stain of hind limb. *=bone lesions. (**F**) H&E stain of osteolytic metastasis (arrows). Scale bar=200um. **(G)** H&E staining of PC9-BrM3 brain metastasis. Scale bars=100um. **(H)** Confocal imaging of H2030-BrM3 cells in the brain (GFP, green), human Ki67 (magenta), CD31+ vasculature (red), and DAPI (blue). Arrows=Ki67 positive tumor cells. Scale bar=23um. **(I)** PC9-BrM3 tumor (GFP, green), surrounded by reactive astrocytes expressing glial fibrillary acidic protein (GFAP, magenta). Scale bar=50um. **J**, H2030 parental and H2030-BrM3 cells were implanted with Matrigel in the lung via intra-thoracic inoculation. Tumors were grown for 6-8 weeks before organs were extracted and imaged. Left: scatter plot of lung photon flux for parental and BrM3 injected mice with a similar range of lung tumor burden. The absence (black dot) or presence (red dot) of brain metastasis is noted for each animal. Representative images of lungs inoculated with parental **(i)** or BrM3 **(ii)** cells and corresponding brains. **(K)** Lung/pleural tumor growth rates were measured following intra-thoracic implantation. Data is presented as the normalized mean lung photon flux. Error bars=SEM. p values based on a two-sided Student's t-test. n=number of animals per cohort.

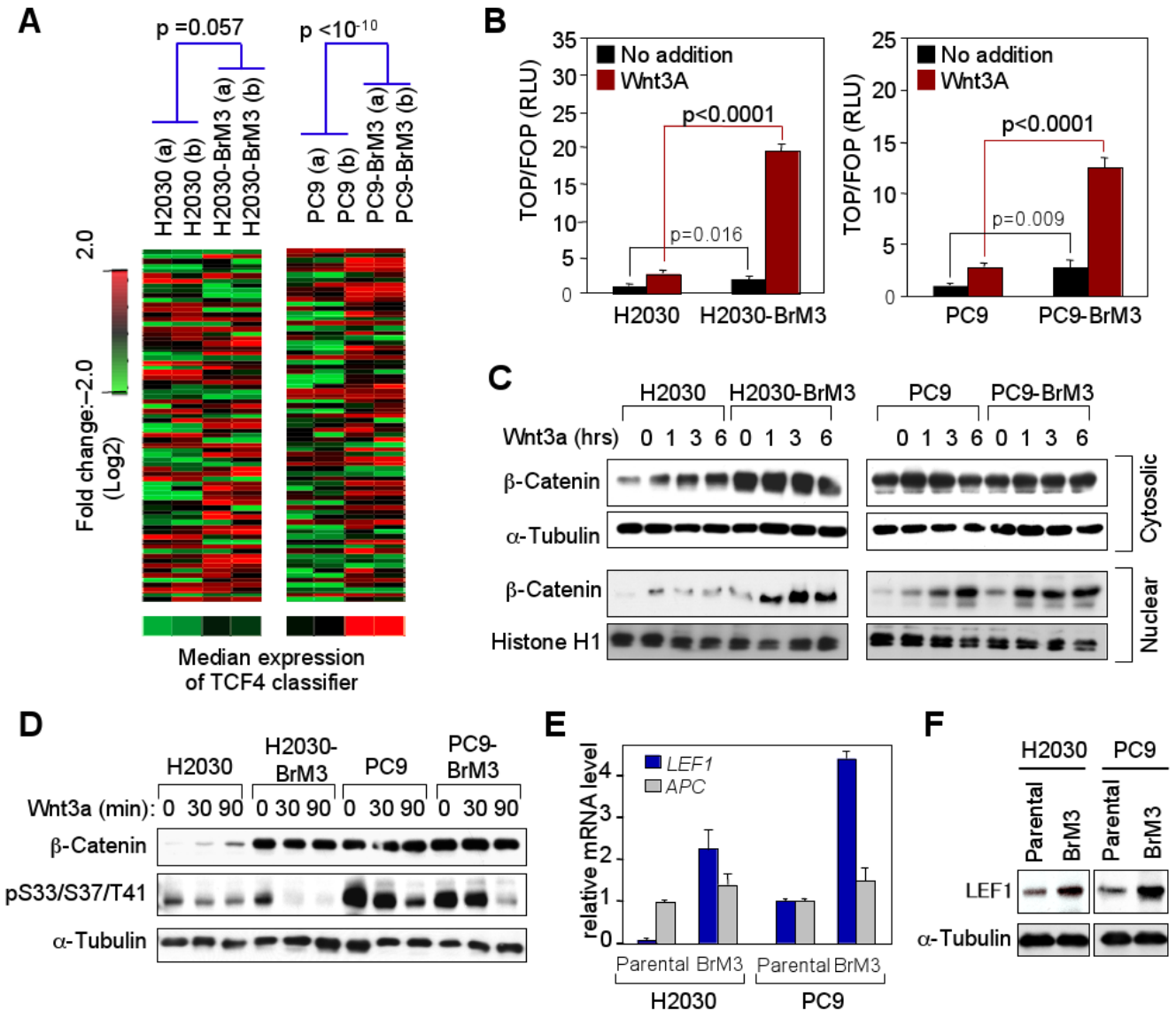

Figure 3. WNT/TCF activity is deregulated in metastatic lung adenocarcinoma cells

(A) Expression of the TCF4 classifier in duplicate samples (a and b) of the indicated derivatives is presented as a heat map. Bottom row represents the median expression of the TCF4 signature. p value from T-test comparing median expression. **(B)** Normalized luciferase measurements of specific TOP-FLASH over non-specific FOP-FLASH activity (TOP/FOP RLU), in derivatives that were mock treated or stimulated with recombinant Wnt3A for 12 hours. Error bars are standard errors of the mean (SEM). p values based on a two-sided Student's t-test. **(C)** Denoted cells were treated with Wnt3a for 0, 1, 3, and 6 hours. Immunoblots were performed for nuclear (top) or cytoplasmic (bottom) β-catenin, α-tubulin, and histone H1. **(D)** Cells were treated with Wnt3a for 0, 30, and 90 minutes. Overall β-catenin protein levels and its ser33/37/Thr41-phosphorylated form were determined by immunoblot. **(E)** Basal expression of *LEF1* and *APC*. Error bars indicate 95% confidence interval from triplicate qRT-PCR samples. **(F)** Immunoblot for LEF1 protein.

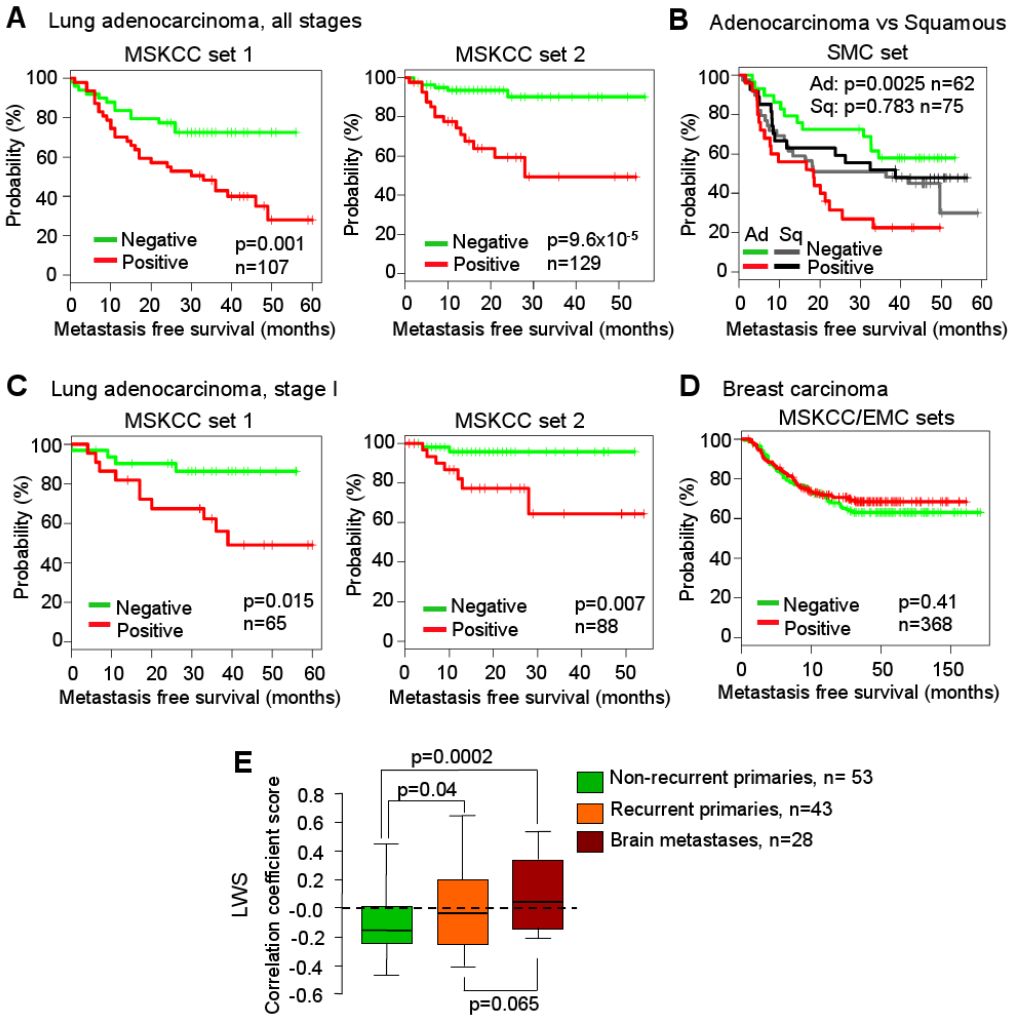

Figure 4. A specific WNT responsive gene set associated with lung adenocarcinoma metastasis

Individual transcriptional predictors from H2030 and PC9 derivatives were obtained by comparing WNT activated to unstimulated cells, and combined to yield the lung cancer WNT responsive gene set (LWS). **(A)** Kaplan-Meier curves for metastasis-free survival based on LWS expression in MSKCC set 1 and MSKCC set 2. Green=LWS negative; red=LWS positive. **(B)** Performance of the LWS in the Samsung Medical Center set (SMC) including a mix of adenocarcinomas and squamous carcinomas of the lung. **(C)** LWS prediction of relapse was observed in stage I lung adenocarcinomas. **(D)** Performance of the LWS in a combined MSKCC-EMC cohort of 368 primary breast cancers. Log rank test was used to determine p-values in A-D. **(E)** The LWS was converted into a Pearson correlation coefficient score that compares the degree of correlation for LWS expression between cell lines activated with Wnt3A, primary adenocarcinomas that included clinical annotation within 5 years (43 recurrences and 53 non recurrences), and 28 brain metastases. Data presented as a Box-whisker plot. p-values calculated by Student t-test.

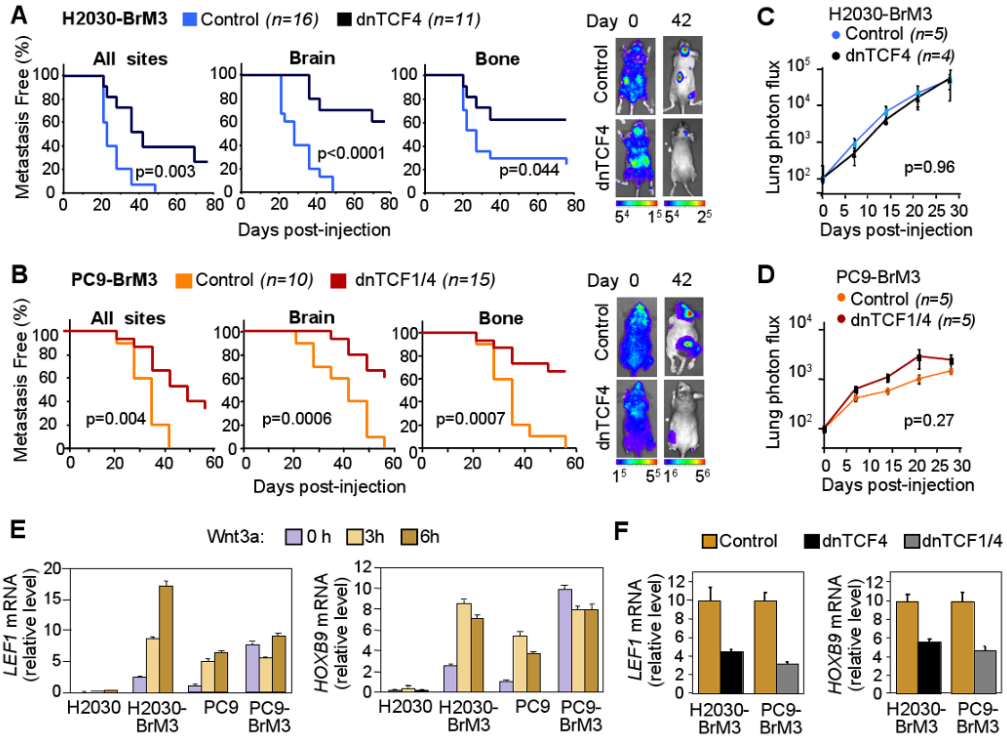

Figure 5. LEF1 and HOXB9 are targets of the metastatic WNT/TCF pathway

(A) Kaplan-Meier curves for metastasis following inoculation of 5×10^4 cells stably expressing an empty vector control or dominant negative TCF4 (dnTCF4), with representative bioluminescent images. **(B)** Control or dnTCF1 and dnTCF4 were expressed in PC9-BrM3 cells. Metastasis was assayed as in A. p-value based on Log rank test. **(C)** Lung tumor growth of H2030-BrM3 cells expressing an empty vector or dnTCF4 as in Figure 2K. **(D)** Similar experiments were performed with control and dnTCF1/4 expressing PC9-BrM3 cells. Error bars=SEM. p values based on a two-sided Student's t-test. **(E)** *LEF1* and *HOXB9* expression were measured via qRT-PCR following Wnt3A stimulation for 0, 3, and 6 hours. Error bars indicate 95% confidence interval from replicates. **(F)** The indicated lines were treated with Wnt3A for 3 hours, and levels of *LEF1* and *HOXB9* determined as in E.

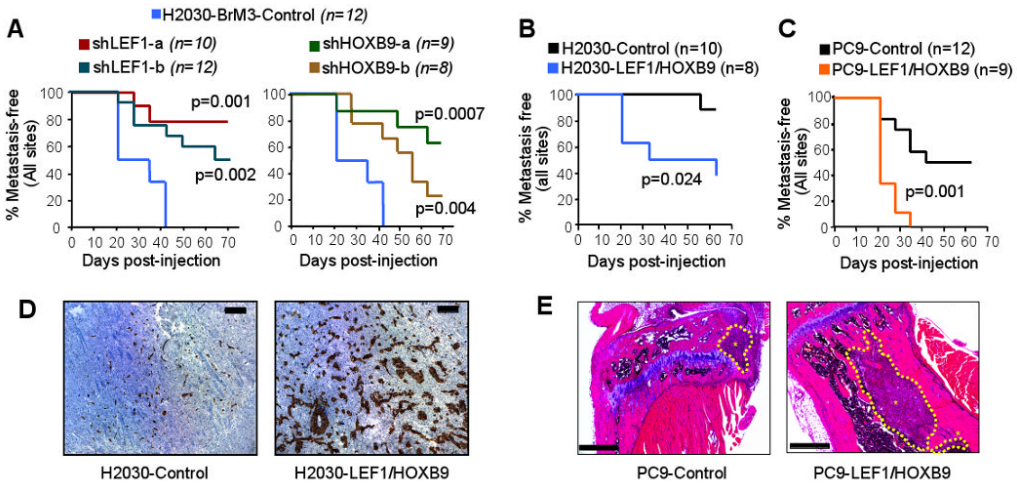

Figure 6. LEF1 and HOXB9 mediate metastasis

(A) Kaplan-Meier curves of overall metastasis incidence, for H2030-BrM3 cells encoding independent hairpins (sh-a and sh-b) against *LEF1* or *HOXB9*. Left: Metastasis in mice inoculated arterially with H2030-BrM3 control, BrM3-shLEF1-a, or BrM3-shLEF1-b cells. Right: H2030-BrM3 control cells versus shHOXB9-a, or shHOXB9-b cells. **(B)** 5×10^4 H2030 parental cells overexpressing either empty vector control or LEF and HOXB9 were inoculated into the circulation of mice, and overall metastasis incidence quantified as in A. **(C)** A similar experiment was performed with PC9 parental lines overexpressing empty vector or LEF1 and HOXB9. **(D)** Brain tissue from animals inoculated with the indicated lines. Brown=GFP^+ tumor foci. Scale= 200um. **(E)** Typical hind limbs extracted from animals inoculated with the indicated lines and that had detectable luminescent signal. *=bone lesion. Scale=500um. p values based on Log rank test.

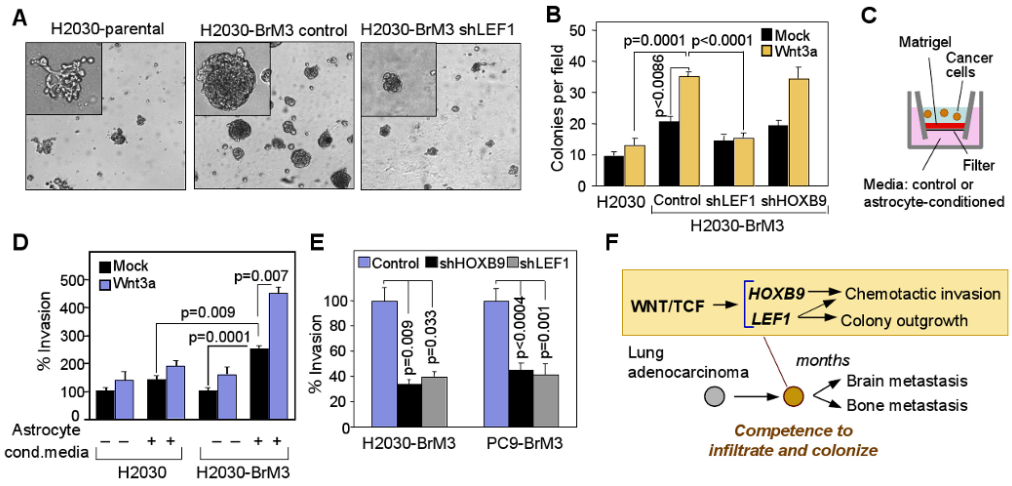

Figure 7. LEF1 and HOXB9 potentiate metastatic outgrowth and chemotactic invasion

(A) The indicated lines were plated into Matrigel and 10X images of colonies captured following 10 days in serum containing media, in the presence or absence of Wnt3a. Inset=representative colonies at 20X. **(B)** Quantification of colonies in the absence (black) or presence (yellow) of Wnt3A. **(C)** Schematic of invasion assay. Parental and metastatic BrM3 cells were mock (black) or Wnt3a stimulated (blue) and seeded into trans-well inserts layered with Matrigel. Assays were performed in the presence of control (-) or astrocytes (+) conditioned media in the bottom chamber. **(D)** Quantification was normalized to the invasion of untreated parental cells. **(E)** Cells were stimulated with Wnt3A and used as in C, with astrocyte chemoattractant. Invasion of the indicated knockdown cells relative to their respective BrM3 control cells. Error bars indicate SEM. p-values calculated based on a two-sided Student's t-test. **(F)** Model depicting the roles of LEF1 and HOXB9 within a WNT/TCF program that drives early multi-organ metastasis in lung adenocarcinoma.